Journal of Imaging Science and Technology® 53(2): 020201–020201-8, 2009.

Monte Carlo Modeling of Light Scattering in Paper

Damir Modrić and Stanislav Bolanča
Faculty of Graphic Arts, University of Zagreb, Zagreb 10000, Croatia
E-mail: damir.modric@grf.hr

Robert Beuc
Institute of Physics, University of Zagreb, Zagreb 10000, Croatia

Abstract. *We introduce a modified Monte Carlo model of light scattering in paper for better understanding of optical dot gain origin. Using a realistic description of paper as a scattering medium and assuming that light distribution in paper (generally any homogeneous or inhomogeneous substrate) depends on its optical properties, we tried to determine light distribution inside paper with known optical properties. In our description, absorption and scattering coefficients of all paper constituents were taken as key functions insofar as they contribute in a real printing application. Due to the fact that paper is a complex medium, it is necessary to involve, in calculations, its surface structure, which was modeled on the base of microfacets. Depicted phenomena were observed and calculated in transmission and reflection. Agreement of the statistical light scattering model in a complex substrate with experimental data demonstrates that the new method successfully describes the phenomena of interest. © 2009 Society for Imaging Science and Technology.*
[DOI: 10.2352/J.ImagingSci.Technol.2009.53.2.020201]

INTRODUCTION

The theory of radiation transmission describes the interaction of radiation with the medium which scatters and absorbs the light. The solutions of radiation transport equations which were obtained during the previous century have been applied to many problems from neutron diffusion, optical tomography, spreading of infra-red and visible light in the atmosphere, and to paper and prints. Initially, the majority of problems of radiation transport were untractable, but with the improvement of mathematical tools and approximations, and as computers become not only available but faster and more powerful, the solutions become more effective and more specialized.

The first approximate solution was given by Schuster[1] who simplified the problem by considering radiation in only the forward and backward directions. Under this author's influence, Kubelka and Munk[2] developed their well-known model.

The original Kubelka–Munk theory was developed for spreading light in parallel colored layers infinitely extended in the *xy* direction[3,4] in order to avoid problems connected with the boundary conditions. The basic assumption of Kubelka–Munk theory is that the layer is uniform and the light distribution within the layer is diffuse. From these assumptions the transport of light in the layer was simplified so that two light flows through the layer were performed, one expanding up and another going simultaneously down along the vertical with respect to the layer. After 1930, when the first paper appeared, Kubelka–Munk theory underwent a series of changes and corrections. At the beginning of the 1940s, Saunderson[5] introduced into the calculation the reflection on the boundary of nearby layers. A few years ago, Emmel[4] and Hersch[6] introduced an elegant mathematical formulation of Kubelka–Munk theory based on matrices. It enables them to apply the Kubelka–Munk theory to images printed in raster reproduction and to treat the optical dot gain. Recently, Mourad[7] extended the representation of Kubelka–Munk theory into three dimensions. Such extension enabled the calculation of light scattering in the substrate and the description of optical dot gain.

The physical phenomenon of optical dot gain or the Yule–Nielsen[8] effect is basically the scattering of light within the substrate (paper) on which some image is printed. Shortly after Yule and Nielsen's publication, Clapper and Yule[9] expand their work by introducing the contribution of multiple internal reflections between the upper and lower boundaries of the substrate. Their supposition was that ink layer was uniform and the light was completely scattered in the substrate. Independently Arney[10] and Hübler[11] suggest in their works similar models based on the statistical description of light scattering.

The present work is focused on solving transient light transport equations by means of the Monte Carlo method. It is a powerful weapon not only for analyzing light transport in turbid media, but also for media such as living tissue, etc. Motivation for applying this simulation was to predict and describe light transport through media such as paper and to investigate its influence on optical dot gain. Based on the work of Wang et al. in 1995,[12] we developed a similar approach to light transport in paper, but optical properties and paper structure require additional approximations and improvements to the initial approach.

In this work we will introduce Monte Carlo path tracing which simulates multiple scattering processes in paper. This method is a numerical technique for solving mathematical problems based on random sampling from well-defined probability distributions.[13,14] As a universal numerical technique, the Monte Carlo method became fully active with the

Received Aug. 18, 2008; accepted for publication Dec. 23, 2008; published online Mar. 6, 2009.
1062-3701/2009/53(2)/020201/8/$20.00.

appearance of computers, and every new computer generation expands the fields of its implementation.

Accordingly one constructs a stochastic model in which an expected variable value (or combination of multiple variables) is equivalent to the value of the required physical quantity. The expected value is usually determined as a mean value of multiple independent samples which reflect the mentioned random variable. To construct a series of independent samples one uses randomly generated numbers which accompany the desired variable distribution. A common approach is to determine macroscopic characteristics of processes in which large numbers of particles participate, such as densities, flows, etc.; individual particle history therein is simulated using random numbers, precise particle interaction probability representation, and an accurate three-dimensional model of problem geometry.

Monte Carlo method simulation of photon propagation offers a flexible yet rigorous approach to photon transfer in a medium such as paper. The method describes local photon propagation rules which are expressed as a probability distribution which, in turn, determines photon step size (mean free path) between two interaction (photon–substrate) points along with the deflecting (scattering) angles from the direction prior to interaction. Due to the fact that this method is statistical and it relies on the calculation of numerous photon paths, it consumes a lot of computer time.

It is essential to emphasize that our simulation does not take into account the wave nature of the light, thereby ignoring wavelength, phase, and polarization. In an exceptionally complex medium as paper, photons suffer multiple scattering events that cause very fast randomization of the phase and polarization which, therefore, do not affect the energy transport significantly.

In the following sections we shall describe the problem we are trying to solve, display how to trace photons in paper, and present comparison between our computational results and measurements. We assume, following light behavior characteristics: linearity, energy conservation, no polarization, no fluorescence, or phosphorescence. Moreover, we assume a steady-state of the system, which means that light distribution is constant in time and is reached instantaneously in real systems.

THEORY

The present method describes the local rules of photon propagation which are expressed, in the simplest case, as the probability distribution of the length of photon free path between two events (interactions with the paper components) and of the scattering angles of the photon.

Paper, as the substrate, is a stochastic three-dimensional structure which consists mainly of fibers, mutually connected by hydrogen bonds on the molecular level, and of the substances which are used as fillers on a macroscopic level. The characteristics of fibers depend on the kind of wood they originate from and the mechanical and chemical treatment during paper production. In the sheet of paper, the individual scattering agents—the fibers and the added particles—are close to one another so that multiple scattering becomes important.

In scattering theory, one starts with the one-fold scattering in which ensembles with sufficiently small particle numbers are studied. Their mutual distance is large enough so that each particle can represent the individual sample without the influence of the neighboring particles. The qualitative criterion for one-fold scattering is that each particle of the ensemble is influenced by the same input electric field with negligible influence from the scattered field owing to other particles in the ensemble. The scattering (absorption) ensemble treatment is such that the scattering (absorption) characteristics ($\bar{K}$) of the ensemble are simply the linear sum of contributions of particular scattering agents[15]

$$\bar{K} = a_1 k_1 + \cdots + a_n k_n, \tag{1}$$

where the coefficient a_i is the statistical weight and k_i is the scattering (absorption) coefficient of ith paper constituent.

Paper is a medium difficult for description because of significant differences in optical characteristics of its components. Approximation of the average scattering function of a particular scattering agent is necessary for applied radiation transfer models and is obtained by means of the old-fashioned Kubelka–Munk theory in its original form. However, this model has recently been noticeably improved by introducing the intensity anisotropy of the propagating diffuse radiation.[16]

The interaction of light with a substance as paper is a complex physical process. Kubelka–Munk theory is a phenomenological one and does not give any information about the actual light scattering in paper. The physical explanation begins with the scattering and absorption of light (photons) on particular particles such as fibers or fillers. Our method is based on macroscopic optical properties of paper components, where we assume that they are uniformly distributed within paper volume. Mean free photon path between interaction positions is within the 10–100 μm interval which satisfies conditions of geometrical optics.

Our approach is based on the work of Phral et al.,[17] where we take into account coating and substrate as two different well-defined layers. We use photon packet instead of a single photon and neglect its phase and polarization.

The optical properties of paper are mainly characterized by three parameters denoted σ_a, σ_s, and g. Interaction of photons with substrate constituent can be defined with absorption and scattering of photons described by the absorption cross-section, σ_a, and the scattering coefficients, σ_s, respectively. So the probability per unit path length of a photon being absorbed or scattered can be summarized to the total interaction coefficient, $\sigma_t = \sigma_a + \sigma_s$, which can be recognized as the Beer–Lambert law. The scattering asymmetry factor, g (also referred to as the anisotropy factor), is defined as the mean value of the cosine of the photon scattering angle. The light scattering properties are mainly influenced by the morphological structure of the paper.

In order to simulate the light transport in a substrate in the Monte Carlo approach, photon packets are sent on a

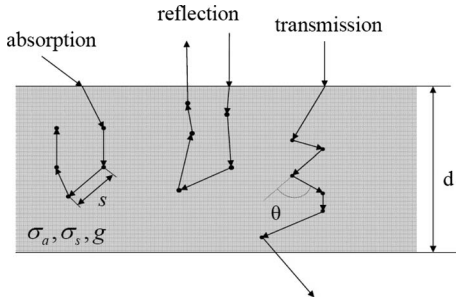

Figure 1. Three possible random walks (absorption, reflection, and transmission as end results of random walk) of a photon in a substrate sample with the optical properties described by σ_a, σ_s, and g, where d is substrate thickness, s is photon packet step size, and θ is scattering angle.

random walk through a virtual paper sample in the computer. The technique is based on probability distributions which describe the main parameters of the photon packet walk which are the free photon packet path between two events (scattering and/or absorption) or photon packet step size, **s**, and scattering angles, ϕ and θ, by means of generating random numbers. Photon packet history (its motion) is recorded until the packet abandons the medium or is absorbed in interaction with the medium (Figure 1). Packets can leave the medium either on the bottom (light transmission) or upper surface (subsurface light transport). When a large amount of photon packets are used, good statistical results of the light distribution in the paper can be obtained.

Photon packet step size **s** is inversely proportional to extinction coefficient or overall attenuation,[17] $\sigma_t = \sigma_a + \sigma_s$, and take values within the interval $s \in [0, \infty)$.

According to the definition of the interaction coefficient σ_t, interaction probability in interval $(s_1, s_1 + ds_1)$ is $\sigma_t ds_1$. It means that light intensity I which has not interacted with medium constituents (paper, filler, coating, etc.) decreases in ds_1 interval according to the Lambert–Beer law

$$\frac{dI(s_1)}{ds_1} = -\sigma_t I(s_1). \tag{2}$$

Variable step size can be determined by means of a probability density function and well known mapping techniques[12,17] where step size is given by means of a random number, $\zeta \in [0, 1]$,

$$s = -\frac{\ln(1-\zeta)}{\sigma_t}. \tag{3}$$

In every interaction point a new direction of the photon packet is obtained. With a new random number ζ, the azimuthal angle $\phi \in [0, 2\pi]$ is calculated by

$$\phi = 2\pi\zeta. \tag{4}$$

The deflection angle θ is a function of the anisotropy coefficient or simply anisotropy, g. The radiation angle distribution can be described by the so-called Henyey–Greenstein[18] phase function what was experimentally proved by Jacques et al.[19] in various tissues. This probability distribution is expressed as

$$p(\cos\theta, g) = \frac{1}{4\pi} \cdot \frac{1-g^2}{\sqrt{[1+g^2-2g\cos\theta]^3}}, \tag{5}$$

where the anisotropy coefficient g is in the range between -1 and 1. Anisotropy coefficient $g=0$ represents the case of isotropic scattering while complete back and forward scatterings are represented by $g=-1$ and 1, respectively. Although paper is not so structurally defined in layers as are tissue samples, we believe that description with the aid of this phase function is valid for our problem.

The deflection angle,[20] θ, can then be determined by using a new random value $\zeta \in (0, 1)$

$$\cos\theta = \begin{cases} \dfrac{1}{2g}\left[1+g^2-\left(\dfrac{1-g^2}{1-g+2g\zeta}\right)^2\right] & \text{for } g \neq 0, \\ 2\zeta - 1 & \text{for } g = 0. \end{cases} \tag{6}$$

Furthermore, we assign an initial weight W to the photon package when it enters the medium. This weight is reduced each time part of the photon packet is absorbed by interaction with the medium. The fraction ΔW (attenuation), subtracted from the initial weight simulating absorption, is given by

$$\Delta W = aW, \tag{7}$$

where a is the albedo $a = \sigma_s/(\sigma_a + \sigma_s)$.

Initial statistical photon packet weight decreases from an initial value of unity during packet propagation through paper and becomes equal to a^n after n steps (events), but it never reaches the limiting value $W=0$. Packets with very small weight are of no physical significance although they continue to propagate within the medium, consuming a great deal of computer time. Because of that, in our simulation a so-called roulette routine is used which terminates the photon packet walk when its weight falls below a particular threshold value and the packet is assumed to be completely absorbed. The process is repeated until the packet leaves the medium or is totally absorbed. After that, a new set of numbers is generated which determines the path and the direction of the new packet.

Our program takes care of the processes occurring when a photon packet hits a boundary between two layers (base and coating) with different optical properties, using Snell's law and Fresnel's formulas.

All numerical simulations presented in this article were done using MathSoft mathematical package MATHCAD 12.

Substrate Modeling

The applied simulation required the most realistic representation possible of paper. Therefore it was necessary to determine real parameters of the medium (paper). In order to get the most relevant data we analyzed the paper cross-section[21] shown in Figure 2. It is an image of a coated paper cross-section obtained with a scanning electron microscope

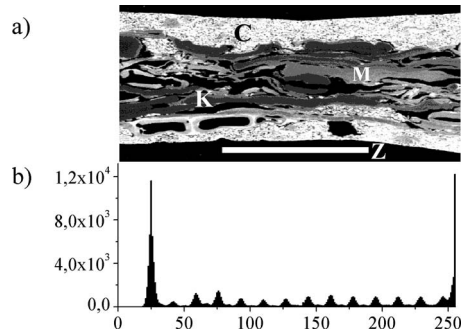

Figure 2. (a) Cross-section of the coated paper with various components: K–chemical pulp, M–mechanical pulp, Z–air (in the original it is the epoxide resin which is used in the production of the microtome cross-sections), and C–coating. The lighter edges in the mechanical and chemical pulp show the binding films.[21] (b) Gray level histogram of the image.

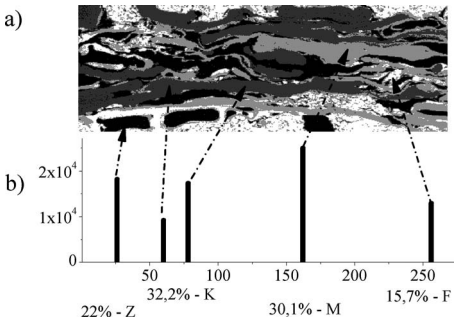

Figure 3. (a) The processed image of four prominent paper base constituents represented with different gray levels; (b) gray level histogram of the image showing percentages of constituents (Z–air, K–chemical pulp; M–mechanical pulp, and F–filler).

(SEM), which has presumed homogeneous coating, uniform depth, and base consisting of two types of fibers (mechanical and chemical pulp) and fillers (gypum, etc.), binders, air, etc. Such an abundance of components is clearly seen from the histogram [Fig. 2(b)] obtained by image analysis with MATHCAD 12 Image Processing Extension Pack. The assignment of paper components represented by corresponding gray level numbers was presented in the Ph.D. dissertation of G. Chinga.[21] In Fig. 2(a), large black regions on the top and bottom of the image are visible which represent air that surrounds the sample, while the white square on the bottom represents a measure bar that equals 50 μm. On the top and bottom of the sample we distinguish a coating layer with irregular geometric structure towards the paper base represented by light tones. In the histogram [Fig. 2(b)] prominent features are in the dark region (around level 25) and light region (around level 255) originating from the surrounding air and coating layer, respectively. Other features in the histogram represent in detail the composition of paper, such as the mechanical and chemical pulp, coating, air, binding films on the edges of pulp fibers, fillers, whiteners, etc.

In order to get improved information about the composition of paper, as well as the percentage representation of a particular component, we had to focus our image analysis on the paper base located in central region of the cross-section (Figure 3).

Grayscale examination of Fig. 3(a), in accordance with gray level assignments in Chinga's work[21] gives us an argument to focus our attention on the main five levels which represent chemical and mechanical pulp, coating, fillers, and air. Careful examination of the mechanical pulp image shows a distinct membrane and, therefore, two gray levels are describing the mechanical pulp. In the analysis of the cross-section image, we applied built-in numerical routines from MATHCAD 12 Image Processing Extension Pack that allow changes in the number of gray levels in an image, and produce an image with n levels (gray scale quantization). In such an approach, choice of the appropriate number of levels can be used for enhancement of the contrast and details of features in an image [Fig. 3(a)]. In our image analysis we generate segmentation by means of visual estimation and determination of associated mean gray level value. The result of analysis is given by the histogram [Fig. 3(b)], where relative intensities in the histogram correspond to percentage component abundance.

In our simulation, photon packet virtual walk through substrate is defined by scattering and/or absorption on all components and is governed by their abundance. Accordingly, corresponding to the constituent percentage in Fig. 3(b), the random number interval [0, 1] was divided into four intervals, each belonging to a specific constituent: air (0–0.22), chemical pulp (0.22–0.542), mechanical pulp (0.542–0.812), filler (0.812–1). In each new step of photon packet walk the generated random number falls into one of these intervals and determines the specific interaction between photon and paper constituent. In this way the interaction of a large number of photon packets with the paper is kept proportional to the statistical distribution of components. It is necessary to emphasize that for each photon step, parameters s, ϕ, and θ were also defined by the generation of related random numbers $\zeta \in [0,1]$.

In Figure 4 two photon packet trajectories are presented which show multiple scattering events (small circles on the graph); while absorption is implied since it cannot be presented graphically. Of course, most of trajectories are not so complex because the packet can leave the substrate after just a few scattering and absorption events. This is clearly demonstrated in Figure 5 where every dot represents one reflected photon packet with the associated weight (relative intensity) in the moment of egress (z-axis) and outgoing position on medium surface (xy-plane). A bell shaped distribution indicates some waste of photon packets, which exit very close to the entrance point with only a slight change in intensity (weight). It can also be seen from Fig. 5 that the intensity distributions of the scattered photon packets for coated and uncoated papers differ in size and dot number, which indicates their different optical properties.

Fig. 5 presents calculated distribution of the scattered photon package intensity as a function of photon packet exit location, where the incident photon beam is perpendicular to paper surface. Each photon packet has 100 photons, what allows us to specify a threshold value of 1%. There is a difference in photon packet intensity distribution for coated

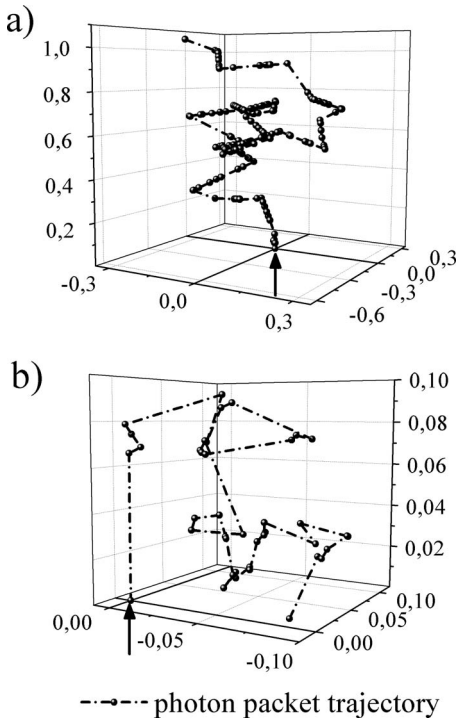

Figure 4. The photon packet trajectory for transmission (a) and reflection (b). Photon packet enters the substrate at point (0,0,0) indicated with black arrows. The arbitrary, relative thickness of the substrate is equal to unity.

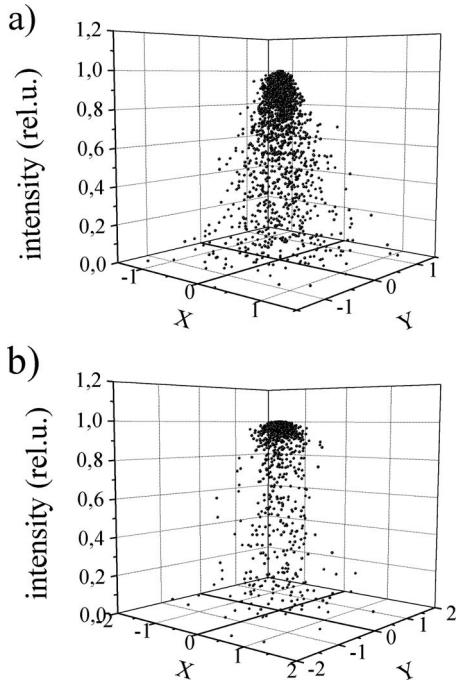

Figure 5. Intensity distribution of the scattered photon packets on incident surface as a function of distance from the entrance location (0,0,0), for uncoated (a) and coated papers (b). Simulation was made for vertical beam incident from above, with 9×10^6 photon packets each containing 100 photons. For the sake of clarity, only a fraction of the dots is presented.

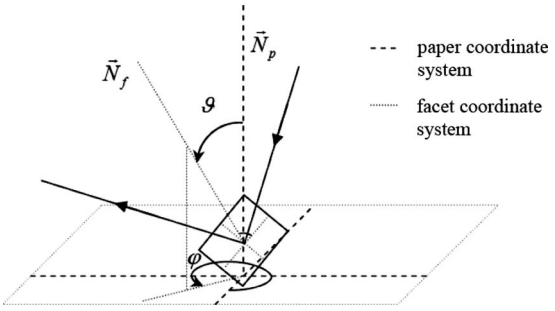

Figure 6. Illustration of microfacet concept of paper surface. The microfacet spatial orientation is defined with two angles, φ and ϑ.

and uncoated paper [Figs. 5(a) and 5(b)] as a consequence of the additional coating layer. The coating has a higher refractive index than paper base components. Therefore, significant numbers of photon packets are reflected on the coating-paper base contact surface which results in broader distribution apex compared to uncoated paper.

Substrate Surface Modeling

Structure of the paper surface demands improvement in the model for more realistic description of the surface itself. Media surface influence has already been investigated and several models (Cook-Torrance, Ward, or Lafortune model) exist. They differ only in determination of the microfacets' tilt distribution. Those rather complicated approaches originated from modeling light scattering in media different from paper such as leather, marble, metal surfaces, etc. In the first approximation we assumed that paper surface is ideally flat and spreads infinitely in the *xy*-plane. Assumption of infinitely extended paper is satisfactory when the thickness of paper is much smaller than surface dimension. Ideal flatness of paper was also a satisfactory approximation for the first estimation of light scattering. Specular reflection calculation from paper surface did not achieve acceptable values, however, owing to the fact that such an approach generates too many photon packets that penetrate the substrate. In order to obtain more realistic values we modeled the paper surface as an area of spatially random oriented microfacets.

Figure 6 illustrates a more realistic description of paper surface. In our simulation, photon packets fall randomly on the paper surface while a large number of packets (10^6 packets) ensures homogeneous covering of the area of interest. Each photon packet falls on one microfacet whose spatial orientation is related to the ideal paper surface in random fashion. The microfacet spatial orientation is defined with two angles $\varphi \in [0, 2\pi]$ and $\vartheta \in [0, \vartheta_g]$. The boundary angle ϑ_g defines paper roughness.

Figure 7 demonstrates that in reality boundary angle ϑ_g value should not exceed 40°. Of course, for glossy papers, the reasonable value is only a few degrees.

RESULTS AND DISCUSSION

All our simulations were carried out for paper containing constituents as described above in Fig. 2. The geometry was such that the one-dimensional photon beam fell vertically to the lower paper surface. Under such conditions there were no specular reflections.

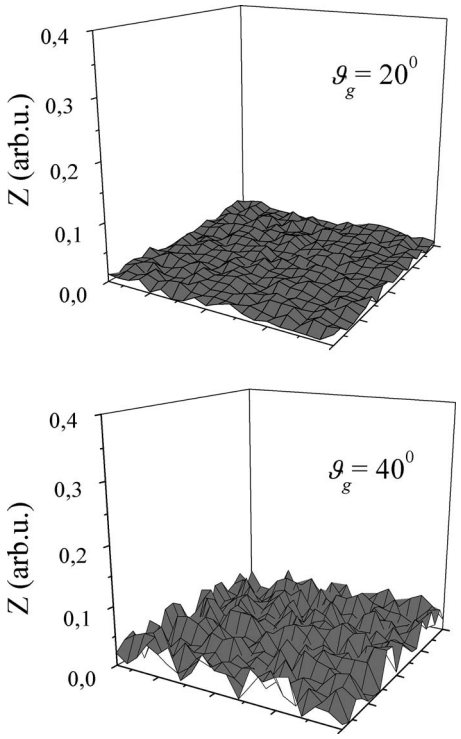

Figure 7. Paper surface modeling with microfacets. Parameter ϑ defines paper surface roughness ($\vartheta \in [0, \vartheta_g]$).

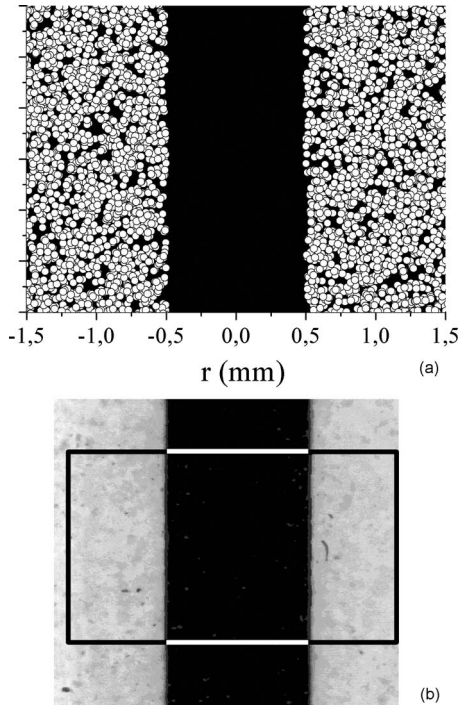

Figure 8. Comparison of theoretical simulation with measurement. (a) Theoretical line simulation, where each dot represents a photon packet exit point. Simulation was performed for 2×10^5 photon packets. (b) Printed line (1 mm) on coated structured paper. Black and white bordered square represents measuring area of PIAS apparatus (region of interest).

Measurements and Data Verification

Our theoretical model was verified by comparison of measured line profiles for various line samples on a test form. The test form was produced on a previously calibrated Indigo Turbo Stream 1000+ digital electrophotographic machine. Analysis of prints was performed with a handheld image analyzer, PIAS[22] introduced by QEA in 2001. These measurements lead to the conclusions that the main source of dot gain is mechanical in nature, and that optical dot gain is small but not negligible.

In our simulation of a printed line square, a photon beam (3 mm width) without a middle region band (1 mm width) was used. The beam consists of 2×10^5 photon packets randomly distributed over the area. The band in the middle without photons represents a nontransparent printed line. Figure 8 presents a comparison of simulated and printed lines. For required analysis printed line was recorded with the PIAS apparatus. The measured line was always thicker than specified (it varies from 4% for a 1 mm line up to 40% for 0.1 mm line) which is typical for several reasons of technical origin: a lateral charge drift in electrophotography; somewhat difficult ink flow in ink jet printers; and positive errors in printer drivers for insurance of full ink coverage of desired areas which is intentional. In our measurement conditions (printing technique, paper–ink combination, and test forms) analysis of printed lines using the PIAS instrument indicate that relative line broadening, which is a consequence of mechanical dot gain caused by ink penetration into the substrate, is constant.

Our results were calculated with typical parameters and components which represent common composition of paper in order to satisfy physical reality and to be simple enough not to consume excessive computer time. All parameters required for calculation are presented in Table I. We applied our model on two types of papers—matte and embossed. In our calculation this was done by applying different angle values, $\vartheta_{g,emb} = 10°$ and $\vartheta_{g,matt} = 35°$ (paper roughness), as parameter values in an algorithm responsible for paper surface structure simulation. Choice of these angles for a fitting parameter was governed by comparison of calculated and measured line reflectance profiles. To introduce the influence of physical dot gain we calculate every reflectance profile for actual line width (measured by PIAS) instead of for nominal line width.

Table I. Paper constituents with their asymmetry factor g, scattering coefficient σ_s absorption coefficient σ_a, and corresponding constituent percentage.[30]

	g–asymmetry factor	σ_s–scattering coefficient (m^2/kg)	σ_a–absorption coefficient (m^2/kg)	Representation percentage (%)
Filler	0.01	55	0.2	12.9
Mechanical pulp	0.8	25	0.3	24.6
Chemical pulp	0.85	55	0.5	26.4
Coating	0.02	300	0.02	18.1
air	0	0	0	18.0

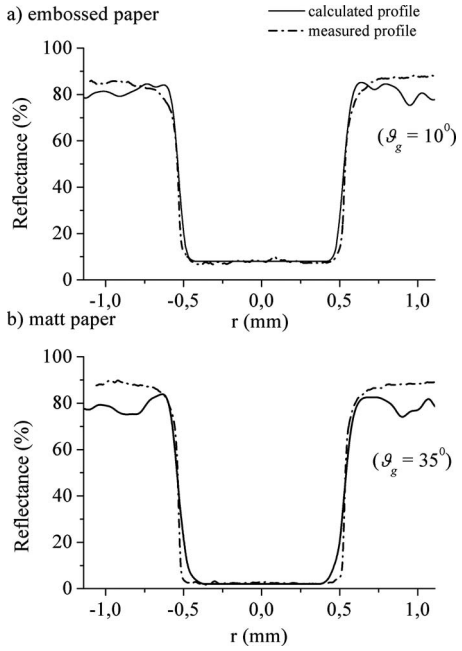

Figure 9. Comparison of calculated and measured reflectance profiles for printed lines of nominal width $d=1$ mm. Profiles were calculated with real (measured) width—d_{st} for embossed and matte paper. Parameter ϑ_g indicates paper surface roughness.

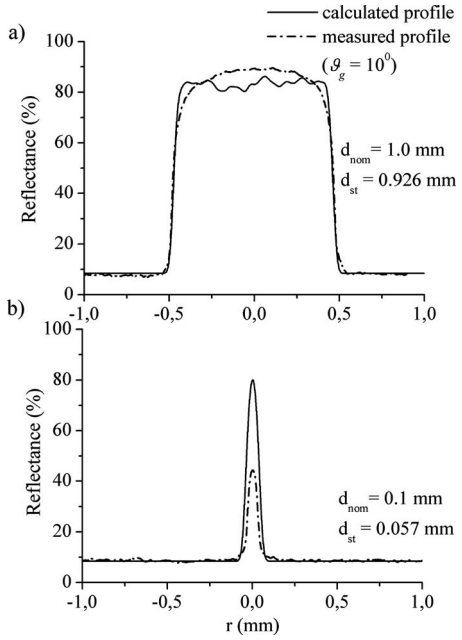

Figure 10. Comparison of calculated and measured line profiles for lines of nominal width $d_{nom}=1$ and 0.1 mm. Profiles were calculated with real (measured) widths—d_{st}. Lines were realized as a space between two solid patches printed on embossed paper.

Light is scattered at interfaces between fibers because the actual fiber walls are essentially transparent. The light scattering coefficient is a measure of interfiber bonding. For the coating we use refractive index $n=1.65$ (barium sulfate or calcium carbonate) and $n=1.55$ (kaolin coating). The refractive index of cellulose fibers is about 1.55, while the corresponding value for typical filler particles is 1.5–2.7, depending on the type of additives used.[23] The scattering coefficient σ_s is large[24,25] and light is highly scattered in paper, while the absorption coefficient of paper is very small.[26] Moreover, the anisotropy factor g of dry paper is typically about 0.8–0.9, which means that paper is predominantly forward scattering material.[27]

In our calculation, a printed raster element area is assumed to be an absorbing element at which the photon packet path terminates. In a forthcoming study we plan to investigate the influence of printed raster element edges on the reflectance profile.

Comparison of calculated and measured line reflectance profiles is shown in Figure 9. There is a better agreement for wider lines whose ratio of line width and dye penetration depth is larger. For finer lines, agreement is fairly good. This conclusion is valid only for printed lines; for lines realized as a space between solid patches (see Figure 10) disagreement is larger for narrower lines (up to 50%), which indicates that the three-dimensional profile of the printed area (dye deposition or diffusion in substrate) is significant and will be investigated in the future. A possible explanation is that dye diffusion in the substrate generates an additional subsurface line boundary which is observed as decreased line width or increased photon packet absorption in that region. Noticeable oscillations observed in the wings of all modeled profiles in areas of maximum reflectance are the consequence of stochastic noise which is determined by the number of incident photon packets (a larger number will generate less oscillation).

CONCLUSIONS

A collective effect called the optical dot gain[28] is affected by scattering and absorption coefficients, type and thickness of coating, substrate, surface structure, ink (physical properties and interaction with substrate), etc. The well-known Kubelka–Munk approach to radiation transfer theory is characterized by bulk scattering and absorption coefficients, but it does not resolve the influence of optical characteristics of paper components on reflectance.

In this article we presented the method for numerical light subsurface scattering simulation based on realistic paper physical characteristics. Validity of the approach was demonstrated by comparison of reflectance profiles of measured and modeled printed raster elements. In consideration of the vast number of photons involved in a real situation (order of magnitude is 10^{23} photons), it was necessary to apply the stochastic approach of the Monte Carlo method. This approach provides plausible results with a large number of trials (in our calculation we deal with 10^9 photons). Each photon can suffer several scatterings and one or none absorptions. Every event (scattering and/or absorption) is described by nine parameters, which significantly increases calculation time and forces us to pay attention to optimization of computer time consumption.

For the printed element where the ratio between line width and penetration depth is large, the model shows good agreement between measured and calculated reflectance pro-

files. Some discrepancy discovered in the case of narrower lines can be attributed to the uncertainty of the line border. Ideally sharp printed lines do not exist due to diffusion of ink in substrate, ink surface tension, changes of ink surface during its desiccation, various technological processes, etc. Realistic line characteristics will be investigated in our future work with special attention to the influence of the raster element border as well as the three-dimensional structure of raster element itself.

In the available literature there is no data for wavelength dependence scattering, absorption coefficients, and asymmetry factors of paper constituents. Therefore, our model is independent of incident light wavelength. Measured wavelength dependence of bulk scattering and absorption coefficients offers no information on behavior of particular constituent coefficients. Nevertheless, introducing wavelength dependence in our model is straightforward and merely awaits proper empirical data.

This model offers the possibility of "experimenting" with various components of paper to obtain desired optical properties without fabricating the real paper itself. This enables verification of certain ideas without time-consuming and expensive paper sample production. Within this approach we can even study optical properties of recycled paper containing residual ink particles and treated components of precursor papers.

Moreover we found that absorption of the paper is much more significant than was previously assumed because of multiple scatterings that cause the attenuation of the photon packet (decrease of weighting). Absorption[29] of the light which penetrates the substrate is, in our calculation, about 30%.

In our calculation influence of scattering asymmetry is negligible because the photon packet, after multiple subsurface scattering, "forgets" information about its initial direction. Randomization of exit photon packet direction in our model is a consequence of random distribution of the cellulose fibers' orientation. In the real situation the cellulose fiber network (paper skeleton) is not entirely randomly oriented, and that will be the subject of future investigations.

ACKNOWLEDGMENT

This work was supported by the Croatian Ministry of Science, Education and Sports under Grant Nos. 035-0352851-3213, 128-1281955-1951, 128-1281955-1960, 128-1281955-1962.

REFERENCES

[1] A. Schuster, "Radiation through a foggy atmosphere", Astrophys. J. **21**, 1–22 (1905) [reprinted in D. H. Menzel, *Selected Papers on the Transfer of Radiation* (Dover, New York, 1966)].
[2] P. Kubelka and F. Munk, "Ein Beitrag zur Optik der Farbanstriche", Z. Tech. Phys. (Leipzig) **11a**, 593–601 (1931).
[3] P. Kubelka, "New contribution to the optics of intensity light scattering materials. Part I", J. Opt. Soc. Am. **38**, 448–457 (1948).
[4] P. Emmel, *Modéles de prédiction couleur appliqués é l'impression jet d'encre*, Thése No. 1857, École Polytechnique Fédérale de Lausanne (1998).
[5] J. L. Saunderson, "Calculation of the color pigmented plastics", J. Opt. Soc. Am. **32**, 727–736 (1942).
[6] R. D. Hersch and P. Emmel, "Towards a color prediction model for printed patches", IEEE Comput. Graphics Appl. **19**, 54–60 (1999).
[7] M. S. Mourad, *Color predicting model for electrophotographic prints on common office paper*, Ph.D. thesis, École Polytechnique Fédérale de Lausanne (2002).
[8] J. A. C. Yule and W. J. Nielsen, "The penetration of light into paper and its effect on halftone reproduction," Proc.-TAGA **3**, 65–76 (1951).
[9] F. R. Clapper and J. A. C. Yule, "The effect of multiple internal reflections on the densities of halftone print on paper", J. Opt. Soc. Am. **43**, 600–603 (1953).
[10] J. S. Arney, "A probability description of the Yule-Nielsen effect. Part I", J. Imaging Sci. Technol. **41**, 633–636 (1997).
[11] A. C. Hübler, "The optical behavior of screened images on paper with horizontal light diffusion", *Proc. IS&T NIP13 Conf.* (IS&T, Springfield, VA, 1997), pp. 506–509.
[12] L. Wang, S. L. Jacques, and L. Zheng, "MCML—Monte Carlo modeling of light transport in multi-layered tissues", Comput. Methods Programs Biomed. **47**, 131–146 (1995).
[13] E. D. Cashwell and C. J. Everett, *A Practical Manual on the Monte Carlo Method for Random Walk Problems* (Pergamon Press, New York, 1959).
[14] I. M. Sobol, *A Primer for the Monte Carlo Method* (Mir, Moskva, 1975).
[15] C. F. Bohren and D. R. Huffman, *Absorption and Scattering of Light By Small Particles* (Wiley, New York, 1983).
[16] W. E. Vargas, "Generalized four-flux radiative model", Appl. Opt. **37**, 2615–2623, (1998).
[17] S. A. Prahl, M. Keijzer, S. L. Jacques, and A. J. Welch, "A Monte Carlo model of light propagation in tissue", in *Dosimetry of Laser Radiation in Medicine and Biology*, (SPIE Institute Series, SPIE, Bellingham, WA, 1989), pp. 102–111.
[18] L. Henyey and J. Greenstein, "Diffuse radiation in the galaxy", Astrophys. J. **93**, 70–83 (1941).
[19] S. L. Jacques, L. Wong, and A. H. Hielscher, "Time-resolved photon propagation in tissues," in *Optical-Thermal Response of Laser Irradiated Tissue*, edited by A. J. Welch and Martin J. C. van Gemert (Plenum Press, New York, 1995).
[20] C. F. Bohren and D. R. Huffman, *Absorption and Scattering of Light by Small Particles* (Wiley, New York, 1983).
[21] G. Chinga, *Structural studies of LWC paper coating layers using SEM and image analysis techniques*, Ph.D. thesis, Norwegian University of Science and Technology, Oslo (2002).
[22] J. C. Briggs, and Ming-Kai Tse, "Objective print quality analysis and the portable personal IAS image analysis system", Nihon Gazo Gakkaishi **44**, 505–513 (2005).
[23] P. Aaltonen, "Paperin optiset ominaisuudet", in *Paperin valmistus*, Vol. 3, edited by A. Arjas (Oy Turun sanomat, Turku, Finland, 1983).
[24] B. Alince, "Light scattering and microporosity in paper", J. Pulp Pap. Sci. **28**, 93–98 (2002).
[25] K. P. Bestem'yanow, "Optical heterodyning study of the propagation dynamics of IR femtosecond laser pulses in a strongly scattering porous medium", Quantum Electron. **34**, 666–668 (2004).
[26] M. Leskelä, "A model for the optical properties of paper, Part 1. The theory", Pap. Puu **75**, 683 (1993).
[27] H. Grandber, *Optical response from paper*, Doctoral thesis, Kungliga Tekniska Högskola, Dept. Production Engineering, Stockholm (2003).
[28] L. Yang and B. Kruse, "Scattering and Absorption of Light in Turbid Media", *IARIGAI' 99* (IARIGAI, Munich, Germany, 1999).
[29] L. Aaltonen and T. Makkonen, "Relationships between mechanical and optical properties of paper affected by web consolidation", in *Transaction of the Symposium on Consolidation of the Paper Web*, edited by F. Bolam (British Paper and Board Makers' Association, London, UK, 1966), pp. 909–927.
[30] W. E. Scott, *Principles of Wet-End Chemistry* (TAPPI Press, Atlanta, GA, 1996), p. 11.